Pollution and Environment (PE)

DOI: http://doi.org/10.7508/pe.01.2023.15.21

ISSN: 2377-5378 (Print)
ISSN: 2377-8148 (Online)
CODEN : PEONAW

ARTICLE

THE IN SITU SYNTHESIS OF Cu_2O-CU POLYHEDRAL HETEROSTRUCTURES AND THE ENHANCED PHOTOCATALYTIC PROPERTIES UNDER VISIBLE LIGHT

Yalin Chen*, Yiyang Wang, Lingfeng Ma, Qian Xu, Bo Ma

School of Materials Science & Engineering, North Minzu University, Yinchuan 750021 China
****Corresponding Author E-mails: Chenyl2023@126.com***

ARTICLE DETAILS

Article History:

Received 2 August 2023
Accepted 5 October 2023
Available online 25 October 2023

ABSTRACT

Energy shortage and environmental pollution have emerged as significant challenges in China's social development. The demand for research and development of efficient new energy materials and the of environmental pollutants in photocatalytic hydrogen production is increasing rapidly. Achieving controllable synthesis of efficient catalytic materials has become a major concern for both domestic and foreign scientists. In this study, Cu_2O-Cu polyhedral heterostructures were synthesized in situ through hydrothermal reaction. The samples were characterized using SEM, TEM, XRD, XPS, and EPR techniques, followed by testing their photocatalytic properties. Experimental results demonstrate that Cu nanoparticles are reduced in situ on the surface of Cu_2O polyhedral particles to successfully construct surface-supported heterostructures. Photocatalytic degradation of methyl orange solution (MO) was conducted under visible light irradiation. Compared to the catalytic degradation rate of 9.8% achieved by Cu_2O particles alone, the photocatalytic performance of Cu_2O-Cu heterogeneous particles further improved with an increase in the number of supported particles reaching a degradation rate of 87.2%. Therefore, the quantity of Cu nanoparticles within Cu_2O-Cu heterogeneous particles plays a crucial role in enhancing their photocatalytic degradation efficiency towards organic matter by improving light absorption characteristics and facilitating effective transfer of photogenerated electrons. This work further provides valuable insights for designing surface-supported photocatalysts.

KEYWORDS

Cuprous oxide; heterostructures; in-situ synthesis; photocatalysis

1. INTRODUCTION

Energy shortage and environmental pollution have become a major problem restricting China's economic and social development. The research and development and preparation of efficient new energy materials and their demand for energy catalysis and environmental pollutant degradation are getting higher and higher [1]. How to achieve controllable synthesis of efficient catalytic materials has become one of the issues of great concern to domestic and foreign scientists. Photocatalysis is a complex process, which involves the steps of light capture, charge separation and molecular adsorption activation. And the most important is the light absorption efficiency and band gap of photocatalytic materials in the water catalytic reaction [2-6]. However, due to the limitation of band gap width and other factors, most semiconductor catalytic materials have some problems, such as weak response to visible light, low photon yield, and difficult to realize large-scale application [7, 8]. The heterogeneous structure can effectively utilize the catalytic active components, mainly due to the mild reaction conditions and efficient interfacial charge transfer, and the rapid electron transfer of multiple channels greatly improves the separation efficiency of charge carriers. As a result of these, the photocatalytic hydrogen production capacity is enhanced [9].

Copper oxide (Cu_2O) crystal is a low-cost and environmentally narrow bandgap semiconductor with a bandgap width of approximately 2.2 eV. It can absorb visible light well and has broad application prospects in fields such as hydrogen production through photolysis of water, photocatalytic degradation of organic compounds, and CO_2 reduction [10-13]. In addition, the geometric diversity and size adjustability of Cu_2O crystals greatly enrich the application of Cu_2O and the selectivity of its composite material design [14, 15]. According to the literature search, Srabanti Ghosh *et al.* formed a heterostructure of Cu-Cu_2O and polypyrrole nanofibers, and good hydrogen production effect was obtained by utilizing the large specific surface area of Cu-Cu_2O heterostructural particles [16]. Dhanasekaran *et al*. produced van der Waals heterostructures composed of layered MoS_2 and WSe_2 on FTO substrate by combining solution bath and RF-sputtering, and confirmed the robustness of electrocatalysis by continuous hydrogen evolution reaction in acidic solution for more than 20 hours [17]. Tabasum *et al*. used the unique electronic and magnetic properties of magnesium oxide heterostructures derived from complex interactions between their electron orbitals, lattice vibrations, and electron spins to contribute to the development of nanoelectronic, spintronic, optoelectronic, and energy storage devices [18]. Santhosh *et al*. prepared ZnO/CdS heterojunctions by chemical precipitation showed better photocatalytic activity and good hydrogen production rate during dye degradation [19]. Zheng *et*

al. successfully synthesized the Z-type heterojunction using HDS-Cu_2O@$CuCo_2O_4$, which showed efficient oxidation and reduction performance the unique shell structure due to the wider visible light response region, reasonable heterojunction interface, and well-matched electronic band structure [20].

In this paper, Cu_2O-Cu polyhedral heterogeneous nanoparticle catalysts were prepared by using copper sulfate pentahydrate, sodium hydroxide, hydroquinone and glucose as raw materials. The hydrothermal react could construct Cu nanoparticles in situ on the surface of Cu_2O polyhedron. Cu particles with different amounts of surface load were obtained by reaction time, and their structure and properties were further characterized and tested. The effect of heterogeneous structures with different nanoparticle loads on catalytic performance was further studied.

2. EXPERIMENT

2.1 Experimental reagents

Cupric sulfate pentahydrate ($CuSO_4 \cdot 5H_2O$), hydroquinone ($C_6H_4(OH)_2$), sodium hydroxide (NaOH), glucose ($C_6H_6O_6$), ethylene glycol ($(CH_2OH)_2$), and anhydrous ethanol were used in this experiment. All the reagents were purchased from Shanghai Aladdin reagent, which were analyzed pure and had not been further purified. Deionized water was used for cleaning during the experiment.

2.2 Preparation of photocatalyst

Firstly, Cu_2O polyhedral particles were synthesized as follows: 0.4996 g copper sulfate pentahydrate ($CuSO_4 \cdot 5H_2O$) was dissolved in 30 ml deionized water to obtain copper sulfate solution. Meanwhile, 1.6 g sodium hydroxide solid was dissolved in 25 ml deionized water to obtain sodium hydroxide solution. Then the copper sulfate solution was placed in a water bath and heated to 55 ℃. The sodium hydroxide solution was added to the copper sulfate solution drop by drop. 5 minutes later, 0.5 g hydroquinone powder was added into. After the reaction for 30 minutes, the obtained brick red precipitate was cleaned, centrifuged, dried and stored for further use.

Then the Cu_2O-Cu polyhedral heterostructural particles were synthesized as follows: First, 20 mg obtained Cu_2O powder above was dispersed ultrasonic in 30 ml glycol solution. Then weighed 2 g sodium hydroxide solid dissolved in 10 ml deionized water to obtain sodium hydroxide solution, and 1.96 g glucose dissolved in 10 ml deionized water to obtain glucose solution. Afterwards, the Cu_2O mixed solution was placed in the water bath and heated to 60 ℃, and the configured sodium hydroxide solution were poured into it step by step. 5 minutes later, the configured glucose solution was poured into. Different loads of Cu_2O-Cu polyhedral heterostructural particles were synthesized after the reaction of 5 minutes, 20 minutes and 60 minutes, respectively. The obtained particles were repeatedly centrifuged, cleaned, dried and stored for further use.

2.3 Sample characterization test

SEM, TEM, XRD, XPS, UV-visible diffuse reflection, PL spectrum, photocurrent response were applied for these samples in characterization and testing.

2.4 Photocatalytic performance test

50 mg sample was evenly dispersed in 50 ml methyl orange solution with a concentration of 10 mg/L, and the sample was fully adsorbed to the methyl orange solution for 30 minutes of dark reaction to achieve the equilibrium state of adsorption-desorption. After the dark reaction, the sample was irradiated by 300 W xenon lamp with 420 nm filter, and a small amount of mixed solution was taken out and filtered at different time. At last, the absorption spectrum of methyl orange solution was measured by ultraviolet spectrophotometer.

3. RESULTS AND DISCUSSION

The Cu_2O-Cu heterostructural particles reacting for 5 minutes, 20 minutes and 60 minutes were named Cu_2O-Cu-5m, Cu_2O-Cu-20m, and Cu_2O-Cu-60m, respectively. In order to determine the microstructure of the prepared samples, SEM was used to observe it, and the results were shown in Figure 1. The Cu_2O sample in Figure 1(a) shows the characteristics of polyhedral particles, including three crystal faces (100), (110) and (111), and the surface is smooth and free of impurities. The Cu_2O-Cu heterostructural particles in Figure 1(b-d) all retain the polyhedral characteristics of Cu_2O particles on the whole, and the in-situ reduced Cu nanoparticles are mainly distributed on the (110) and (111) crystal faces with large crystal surface energy. In the sample of Cu_2O-Cu-5m, a small amount of Cu particles appear on the surface of Cu_2O particles, and their distribution is uneven. In the samples of Cu_2O-Cu-20m, the Cu

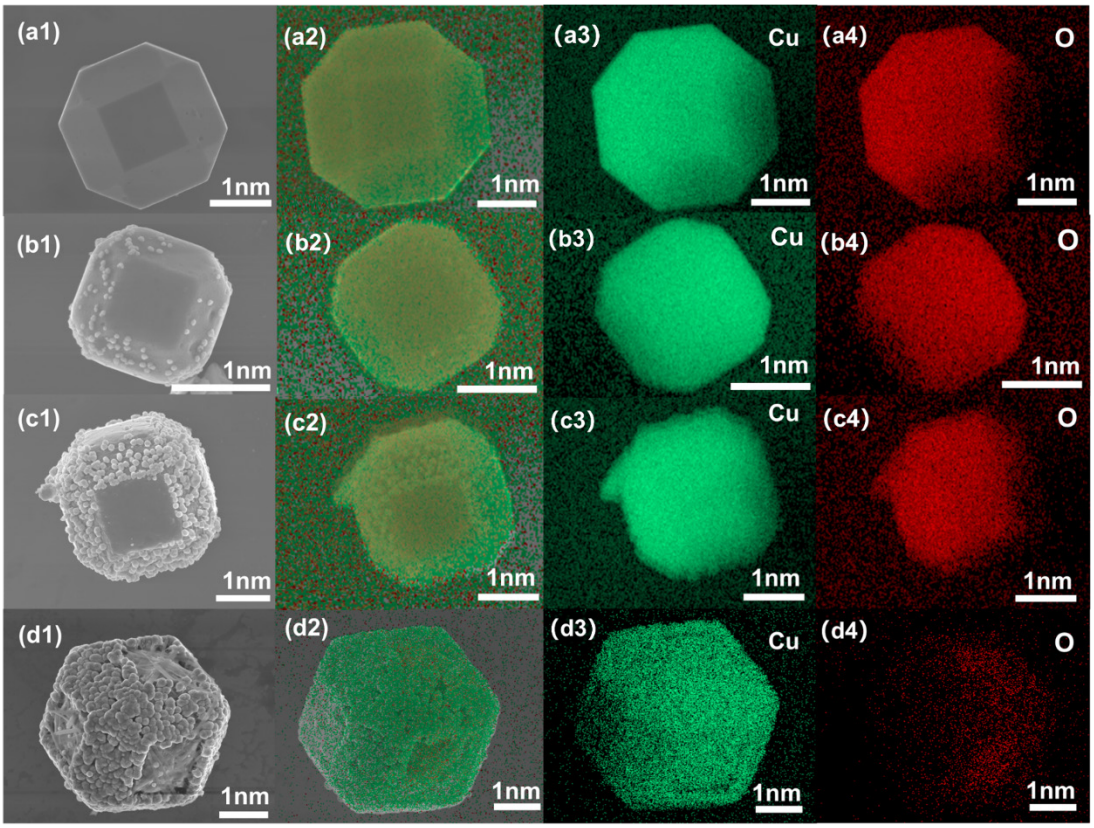

Figure 1. SEM and element mapping images of individual particles, (a) Cu_2O; (b) Cu_2O-Cu-5m; (c) Cu_2O-Cu-20m; (d) Cu_2O-Cu-60m.

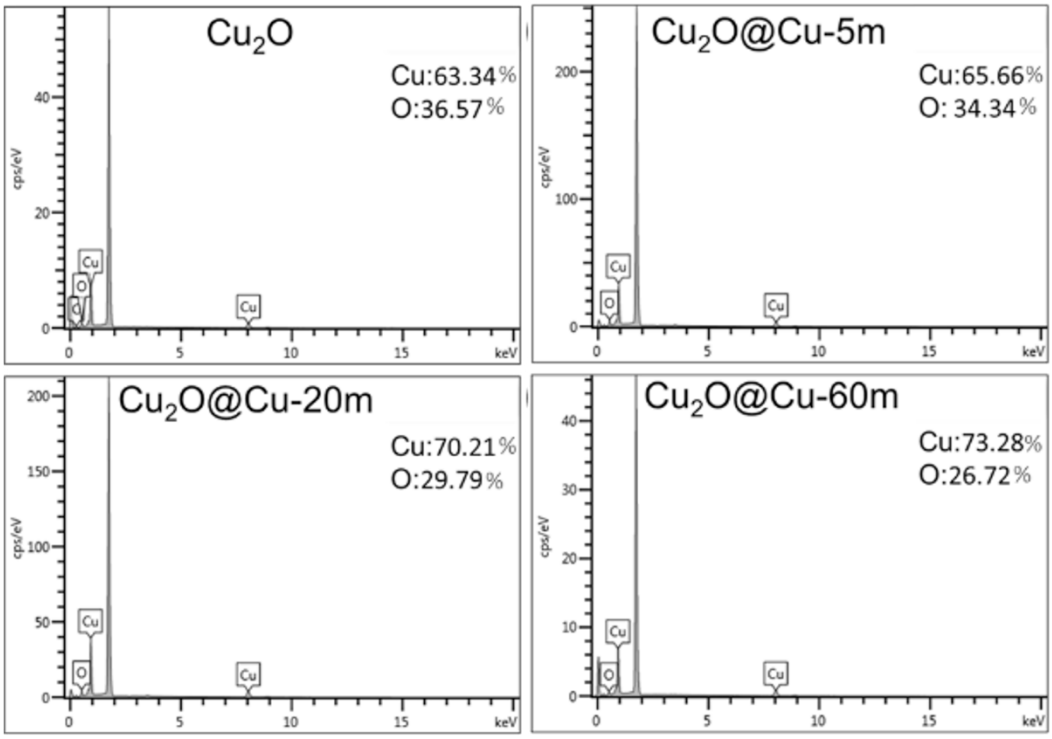

Figure 2. EDS of different Cu_2O-Cu polyhedral heterostructures.

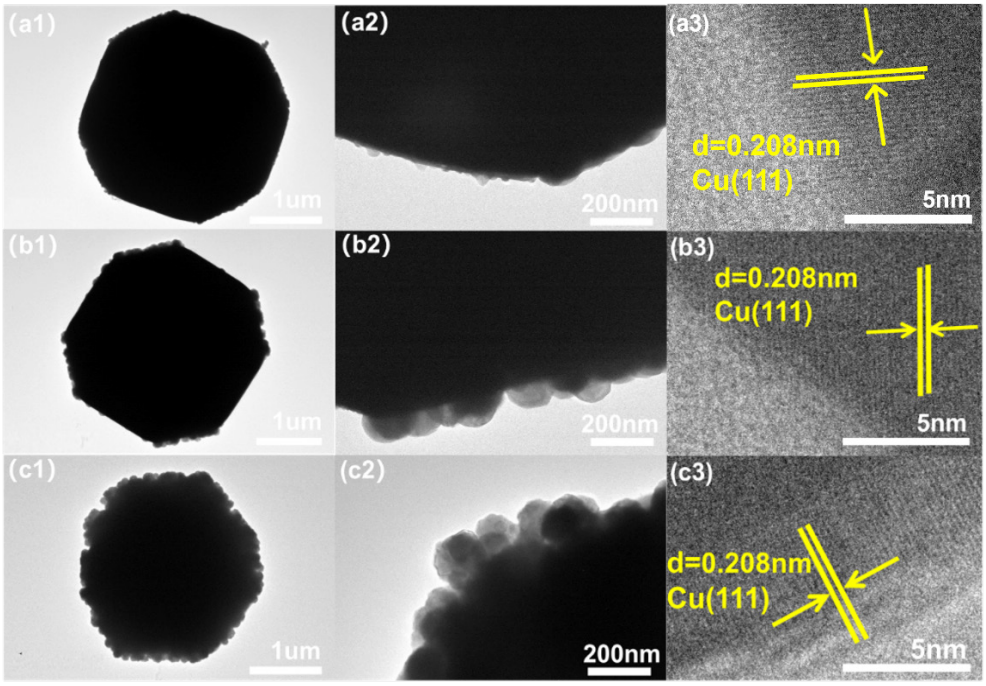

Figure 3. High magnification TEM and HRTEM of different Cu_2O-Cu polyhedral heterostructures, (a) Cu_2O-Cu-5m; (b) Cu_2O-Cu-20m; (c) Cu_2O-Cu-60m.

particles on the surface of Cu_2O particles increase obviously. In Cu_2O-Cu-60m samples, the diameters of Cu particles increase, and the (110) and (111) crystal surfaces of Cu_2O polyhedral particles are covered with full layers of Cu nanoparticles. At the same time, the element distribution analysis was carried out. It indicates that both Cu and O elements were detected, and more copper elements were distributed on the surface.

In order to further clarify the element types and relative contents in each sample, EDS spectrum analysis was carried out. As shown in Figure 2, Cu and O elements were detected in all samples, and the content of Cu element in Cu_2O, Cu_2O-Cu-5m, Cu_2o-Cu-20m and Cu_2O-Cu-60m samples gradually increased, while the content of O element gradually decreased. Therefore, the above characterization results certificate that the particles loaded on the surface of Cu_2O are in-situ reduced Cu particles, and no other impurity particles are introduced.

The surface-loaded particles in the heterogeneous structures were characterized by TEM and HRTEM, and the results were shown in Figure 3. The in-situ reduction of Cu nanoparticles from the surface of Cu_2O particles can be observed in all three samples of Cu_2O-Cu-5m, Cu_2O-Cu-20m and Cu_2O-Cu-60m. It can be obviously observed that with the extension of reaction time, the Cu nanoparticles on the surface of Cu_2O particles are gradually reduced to the surface, and the particle diameter also increases gradually. Cu_2O-Cu-60m particles are the most obvious, which is consistent with the results obtained by SEM. In the HRTEM image, it can be observed that the lattice fringe spacing on the surface of the prepared sample is 0.208 nm, corresponding to the (111) crystal surface of Cu, which further proves that the prepared particles are heterostructures composed of Cu particles reduced in situ on the surface of Cu_2O particles.

In order to determine the phase composition and crystal structure of the prepared samples, the samples were characterized by XRD patterns. As shown in Figure 4(a), the prepared Cu_2O has an obvious cubic crystal structure at 29.5°, 36.4°, 42.3°, 52.4°, 61.3°, 69.5°, 73.5° and 77.3°, corresponding to (110), (111), (200), (211), (220), (310), (311) and

(222) crystal faces. For the Cu_2O-Cu polyhedral heterostructures, both Cu_2O and Cu exist in the product, and the diffraction peaks of Cu in the sample gradually increase with the increase of reaction time. Concretely, Cu_2O-Cu-5m has no obvious (111) diffraction peak, and Cu_2O-Cu-20m can see a weak diffraction peak in the XRD pattern. However, Cu_2O-Cu-60m can see an obvious Cu (111) diffraction peak in the XRD pattern.

XPS characterization was performed to explore the composition and valence states of elements in these samples. According to the XPS full spectrum in Figure 4(b), in addition to the characteristic peaks of element C, only the characteristic peaks of elements Cu and O were observed in the sample, further demonstrating that the method did not introduce other impurity particles during in-situ reduction to prepare heterogeneous structures. It can be observed from Figure 4(c) that for the three Cu_2O-Cu heterostructures, obvious Cu 2p diffraction peaks located at 932.3 eV and 952.4 eV were detected, which is correspond to Cu^{1+}. However, since the positions of Cu 2p diffraction peaks for Cu^{1+} and Cu^0 are very close, they cannot be distinguished. So the LMM

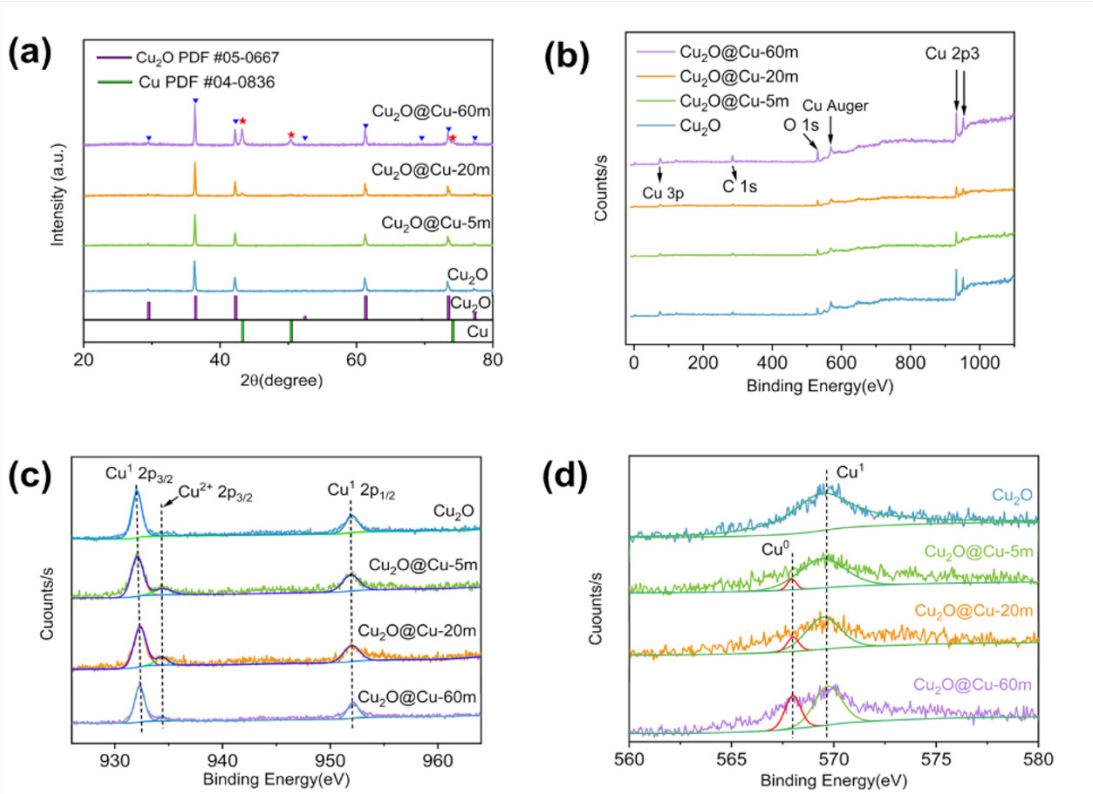

Figure 4. Samples of different Cu_2O-Cu (a) XRD; (b) XPS of full spectrum; (c) XPS of Cu 2p, and (d) XPS of Cu LMM.

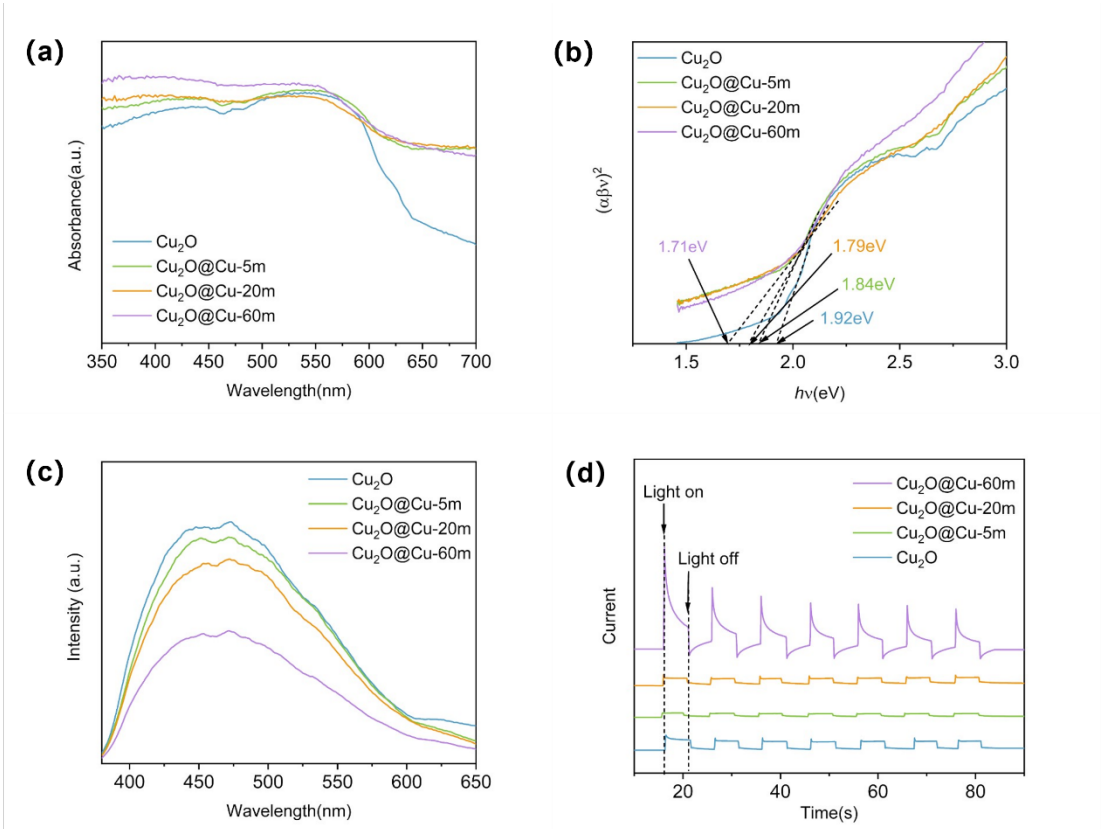

Figure 5. (a) UV-visible light diffuse reflection spectrum map of different in-situ Cu_2O-Cu samples; (b) the corresponding band gap; (c) the photoluminescence spectrum; (d) diagram of the photocurrent response generated under visible light.

diffraction peaks of Cu elements were further detected. As shown in Fig. 4(d), Cu_2O particles only have the characteristic diffraction peak of Cu^{1+} at 569.6 eV. Nevertheless, all the three heterogeneous particles have another characteristic diffraction peaks of Cu^0 at 568.1 eV, and the diffraction intensity is gradually enhanced. The rusutl indicates that the prepared heterogeneous particles have achieved in-situ reduction of Cu nanoparticles, and the controlled synthesis of Cu_2O-Cu polyhedral heterostructural particles with different loading capacities was formed [21].

The optical properties of catalysts are also important factors to evaluate their photocatalytic activity. The light absorption of the sample was studied through the characterization of UV-visible light diffuse reflection. It can be seen from Figure 5(a) that the four samples all have satisfying light absorption characteristics for the visible region. The order of the absorbed light intensity of the four samples from small to large is Cu_2O, Cu_2O-Cu-5m, Cu_2O-Cu-20m, Cu_2O-Cu-60m. The relation curve of $(\alpha h\nu)^2$-$h\nu$ can be obtained by converting the spectrum, and the corresponding bandgap diagram can be drawn. As shown in Figure 5(b), the calculated bandgap width of Cu_2O, Cu_2O-Cu-5m, Cu_2O-Cu-20m and Cu_2O-Cu-60m are 1.92eV, 1.84eV, 1.79eV and 1.71eV respectively, indicating that the loaded Cu nanoparticles can effectively reduce the band gap width of Cu_2O. In Figure 5(c), PL spectrum test was performed on the sample, and the results showed that the emission spectral intensity of Cu_2O-Cu heterogeneous particles is lower than that of Cu_2O polyhedral particles. This result ensures that the charge separation efficiency of Cu_2O-Cu in situ supported heterostructures is improved, which is consistent with the above characterization [22]. The photocurrent response under visible light had been tested in Figure 5(d). It indicates that the photocurrent density and intensity also increase successively, which proves that heterostructures can generate more photogenerated carriers in the photocatalytic reaction and have higher photogenerated carrier separation efficiency. It is worth noting that the Cu_2O-Cu-60m sample with the largest loading capacity shows the best performance in light absorption characteristics, band gap width regulation, PL fluorescence intensity, and photocurrent response. This sample indicates that the more loaded particles, the more obvious the optical performance improvement of heterogeneous structures.

In order to determine the catalytic activity of Cu_2O-Cu sample, the photocatalytic reaction kinetics of Cu_2O-Cu on methyl orange (MO) solution was studied. As shown in Figure 6(a), after the photo-degradation for 90 min, the photocatalytic degradation efficiency of Cu_2O, Cu_2O-Cu-5m, Cu_2O-Cu-20m and Cu_2O-Cu-60m for MO were 1.1%,9.8%,26.7% and 87.2%, respectively. The order of degradation efficiency is consistent with the results of the above optical properties. It suggests that the photocatalytic performance of Cu_2O-Cu in situ supported heterostructures is significantly improved compared with Cu_2O particles, and Cu_2O-Cu-60m shows the best photocatalytic performance. Figure 6(b) shows the kinetic fitting diagram of photocatalytic degradation process of different catalysts. The calculation formula is as follows [23]:

$$\ln\frac{C}{C_0} = -kt \quad (1)$$

The rate constants of Cu_2O, Cu_2O-Cu-5m, Cu_2O-Cu-20m and Cu_2O-Cu-60m are -7.79×10^{-4}, 3.30×10^{-4}, -2.7×10^{-3} and -1.7×10^{-2} min^{-1}, respectively. The rate constant of Cu_2O-Cu-60m is the largest, which proves that Cu_2O-Cu-60m has the best photocatalytic effect.

EPR tests were performed on four samples to determine the active substance in the reaction. As shown in the Figure 7, with the increase of the number of supported Cu nanoparticles, •OH and $\bullet O_2^-$ have obvious signal peaks under visible light irradiation, and the intensity is gradually increased, indicating that •OH and $\bullet O_2^-$ and as active substances participate in the reaction in the photocatalytic reaction. Moreover, the more Cu nanoparticles supported on the surface, the stronger the separation effect of photogenerated electron pairs, and the more active substances. This result is consistent with the above results of photocatalytic degradation of methyl orange.

Finally, the mechanism of photocatalytic performance improvement of Cu_2O-Cu heterogeneous particles was analyzed. As shown in Figure 8, since the Fermi level of Cu_2O is lower than that of Cu, when the two materials form a heterostructure, a thermodynamic equilibrium is required [24]. Then the Fermi level of Cu moves downward and the Fermi level of Cu_2O moves upward, and a new heterostructure E_f is constructed. At this time, when the heterostructural catalyst is irradiated with visible light, the electrons in the Cu_2O valence band (VB) will be excited to the conduction band (CB), and the corresponding number of photogenerated holes will be generated at the original Cu_2O VB. However, since the

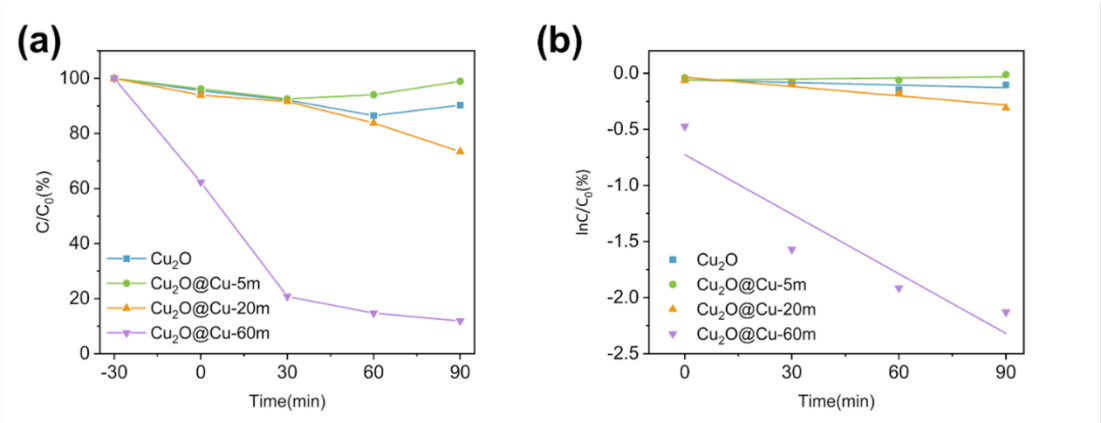

Figure 6. (a) Degradation plot of methyl orange solution under visible light of different Cu_2O-Cu. (b) The corresponding kinetic k values.

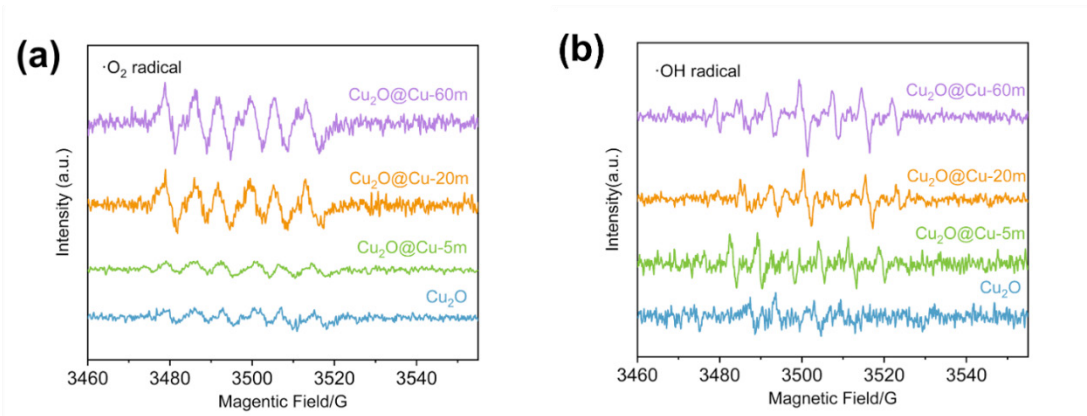

Figure 7. EPR detection of •OH radicals and $\bullet O_2^-$ radicals for different samples.

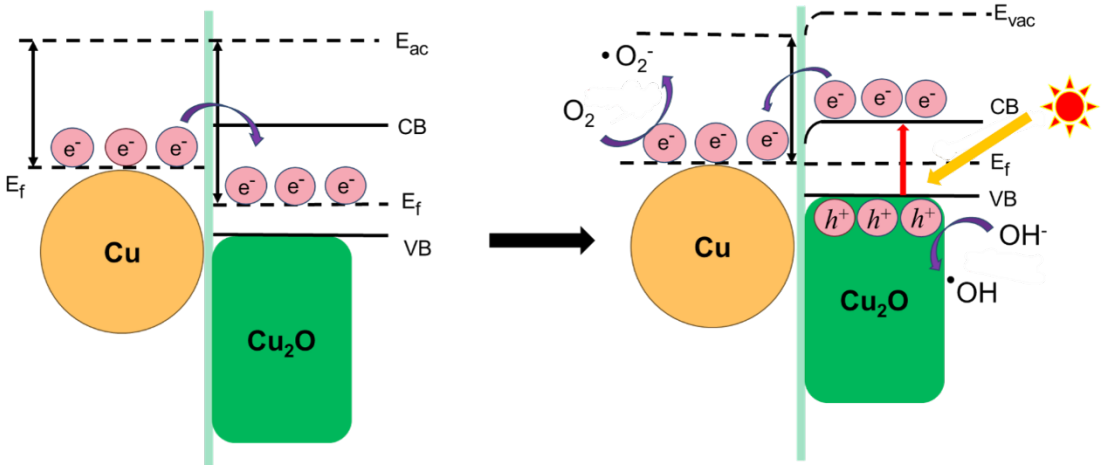

Figure 8. Mechanism diagram of the photocatalytic performance enhancement.

electrons in CB is not in a stable state, these excited electrons will be transferred to the surface of the Cu particles. Thus, a large number of photogenerated electrons are accumulated on the Cu particles. Due to the action of Schottky barrier, the holes of Cu_2O VB cannot be transferred to the surface of Cu nanoparticles, thus realizing the effective separation of electron hole pairs. The more Cu nanoparticles on the surface of Cu_2O, the more sites to receive photogenerated electrons, and the separation efficiency of electron holes will be further improved, so the Cu_2O-Cu-60m heterostructure shows the best photocatalytic performance. Finally, the photogenerated electrons gathered on the surface of the Cu nanoparticles are captured by O_2 to generate $\bullet O_2^-$, and the holes remaining in the valence band of Cu_2O are captured by OH^- to form •OH. The two active substances degrade the organic dyes into harmless substances such as water.

4. CONCLUSIONS

In situ reduction of Cu nanoparticles on the surface of Cu_2O polyhedral particles was achieved by a simple hydrothermal method, and then Cu_2O-Cu polyhedral heterogeneous photocatalyst with different loading loads was prepared. The results showed that with the increase of reaction time, the Cu nanoparticles were uniformly distributed on the (111) and (110) crystal surfaces with high surface activity of Cu_2O polyhedron. When the Cu nanoparticles formed thin shells and load on the crystal surfaces of the Cu_2O polyhedron, heterogeneous particles had the best photocarrier separation efficiency. The photocatalytic degradation efficiency of methyl orange dye under visible light can reach 87.2%, which is significantly higher than that of unloaded Cu_2O polyhedral particles. Therefore, the number of Cu nanoparticles in heterogeneous structures plays a crucial role in photocatalytic degradation of organic matter. They can enhance the light absorption characteristics of the particles and effectively promote the transfer of photogenerated electrons, which provides a research idea for the design of surfacing supported photocatalysts.

ACKNOWLEDGMENTS

This work was supported by the Natural Science Foundation of Ningxia (No. 2022AAC03225), the Fundamental Research Funds for the Central Universities, North Minzu University (No. 2021KYQD02), and the Innovation Training Project for College Students (No. S202211407001).

REFERENCES

[1] Hou, J., Wu, Y., Zhang, B., Cao, S., Li, Z., Sun, L. 2019. Rational Design of Nanoarray Architectures for Electrocatalytic Water Splitting. Advanced Functional Materials, 29 (20), 1808367.

[2] Wang, B., Zhang, W., Zhang, Z., Li, R., Wu, Y., Hu, Z., Wu, X., Guo, C., Cheng, G., Zheng, R. 2016. Cu2O Hollow Structures—Microstructural Evolution and Photocatalytic Properties. RSC Advances, 6 (105), 103700.

[3] Yu, C., Shu, Y., Zhou, X., Ren, Y., Liu, Z. 2018. Multi-branched Cu2O Nanowires for Photocatalytic Degradation of Methyl Orange. Materials Research Express, 5 (3), 035046.

[4] Chang, J., Bao, Q., Zhang, C., Zhao, X., Cao, Z., Wang, Y., Li, R., Guo, R., Li, H., He, J. et al. 2021. Rapid Preparation and Photocatalytic Properties of Octahedral Cu2O@Cu Powders. Advanced Powder Technology, 32 (1), 144.

[5] Chamorro-Mena, I., Linares, N., García-Martínez, J. 2023. Blue-LED ACTIVATED PHOTOCATALYTIC HYDROGENATION of NITROARENES with Cu2O/CuO HETEROJUNCTIONS. Dalton Transactions, 52 (37), 13190.

[6] Kumar, S., Bhawna, Gupta, A., Kumar, R., Bharti, A., Kumar, A., Kumar, V. 2023. New Insights into Cu/Cu2O/CuO Nanocomposite Heterojunction Facilitating Photocatalytic Generation of Green Fuel and Detoxification of Organic Pollutants. The Journal of Physical Chemistry C, 127 (15), 7095.

[7] Li, J., Li, J., Chen, Q., Bai, J., Zhou, B. 2013. Converting Hazardous Organics into Clean Energy Using A Solar Responsive Dual Photoelectrode Photocatalytic Fuel Cell. Journal of Hazardous Materials, 262, 304.

[8] Ovcharov, M. L., Mishura, A. M., Shcherban, N. D., Filonenko, S. M., Granchak, V. M. 2016. Photocatalytic Reduction of CO2 Using Nanostructured Cu2O with Foam-Like Structure. Solar Energy, 139, 452.

[9] Li, N., Yan, W., Niu, Y., Qu, S., Zuo, P., Bai, H., Zhao, N. 2021. Photoinduced in Situ Spontaneous Formation of a Reduced Graphene Oxide-Enwrapped Cu–Cu2O Nanocomposite for Solar Hydrogen Evolution. ACS Applied Materials & Interfaces, 13 (8), 9838.

[10] Lou, Y., Zhang, Y., Cheng, L., Chen, J., Zhao, Y. 2018. A Stable Plasmonic Cu@Cu2O/ZnO Heterojunction for Enhanced Photocatalytic Hydrogen Generation. ChemSusChem, 11 (9), 1505.

[11] Yu, X., Kou, S., Zhang, J., Tang, X., Yang, Q., Yao, B. 2018. Preparation and Characterization of Cu2O Nano-Particles and Their Photocatalytic Degradation of Fluroxypyr. Environmental Technology, 39 (22), 2967.

[12] Su, Q., Zuo, C., Liu, M., Tai, X. 2023. In Molecules, 28.

[13] Zhu, H., Xi, M., Huang, G., Qin, L., Zhang, T., Kang, S.-Z., Xiangqing, L. 2023. Cuprous Oxide Core-Shell Heterostructure Facilely Encapsulated by Cadmium Metal Organic Frameworks for Enhanced Photocatalytic Hydrogen Generation. Journal of Physics and Chemistry of Solids, 181, 111476.

[14] Song, S. H., Hong, S., Cho, M., Yoo, J.-G., Min Jin, H., Lee, S.-H., Avdeev, M., Ikeda, K., Kim, J., Nam, S. C.et al. 2022. Rational Design of Li Off-Stoichiometric Ni-Rich Layered Cathode Materials for Li-ion Batteries. Chemical Engineering Journal, 448, 137685.

[15] Ghodselahi, T., Vesaghi, M. A., Shafiekhani, A., Baghizadeh, A., Lameii, M. 2008. XPS Study of the Cu@Cu2O Core-Shell Nanoparticles. Applied Surface Science, 255 (5, Part 2), 2730.

[16] Ghosh, S., Keshri, S. R., Bera, S., Basu, R. N. 2020. Enhanced Solar

Hydrogen Generation Using Cu–Cu2O Integrated Polypyrrole Nanofibers as Heterostructured Catalysts. International Journal of Hydrogen Energy, 45 (11), 6159.

[17] Vikraman, D., Hussain, S., Truong, L., Karuppasamy, K., Kim, H.-J., Maiyalagan, T., Chun, S.-H., Jung, J., Kim, H.-S. 2019. Fabrication of MoS2/WSe2 Heterostructures as Electrocatalyst for Enhanced Hydrogen Evolution Reaction. Applied Surface Science, 480, 611.

[18] Huma, T., Hakimi, N., Younis, M., Huma, T., Ge, Z., Feng, J. 2022. In Nanomaterials, 12.

[19] Nadikatla, S. K., Chintada, V. B., Gurugubelli, T. R., Koutavarapu, R. 2023. In Molecules, 28.

[20] Zheng, J., Liu, X., Zhang, L. 2020. Design of Porous Double-Shell Cu2O@CuCo2O4 Z-Scheme Hollow Microspheres with Superior Redox Property for Synergistic Photocatalytic Degradation of Multi-Pollutants. Chemical Engineering Journal, 389, 124339.

[21] Jo, M., Tanaka, A. 1996. Auger Electron Peaks of Cu in XPS. Applied Surface Science, 100-101, 11.

[22] Ren, G.-X., Yu, B., Liu, Y.-M., Wang, H.-X., Zhang, W.-G., Liang, W. 2017. High Photocatalytic Activity of Cu2O/TiO2/Pt Composite Films Prepared by Magnetron Sputtering. Rare Metals, 36 (10), 821.

[23] Wu, Q., Liu, X., Hou, S., Qiang, L., Zhang, K., Yang, Z. 2021. Biotemplate Synthesis and Photocatalysis Performance of Multilayer Porous ZnWO4 Nano-Photocatalyst with Rose Petals as Template. Colloids and Surfaces A: Physicochemical and Engineering Aspects, 629, 127459.

[24] Song, W., Ma, S., Wang, L., Liu, J., Zhao, Z. 2017. Theoretical Explanation of the Photogenerated Carrier Separation at the Surface Junction. ChemCatChem, 9 (23), 4340.